HHS Public Access

Author manuscript

Cell Metab. Author manuscript; available in PMC 2016 July 07.

Published in final edited form as:

Cell Metab. 2015 July 7; 22(1): 86–99. doi:10.1016/j.cmet.2015.05.012.

A periodic diet that mimics fasting promotes multi-system regeneration, enhanced cognitive performance and healthspan

Sebastian Brandhorst[1,†], **In Young Choi**[1,†], **Min Wei**[1], **Chia Wei Cheng**[1], **Sargis Sedrakyan**[2], **Gerardo Navarrete**[1], **Louis Dubeau**[3], **Li Peng Yap**[4], **Ryan Park**[4], **Manlio Vinciguerra**[5], **Stefano Di Biase**[1], **Hamed Mirzaei**[1], **Mario G. Mirisola**[6], **Patra Childress**[7], **Lingyun Ji**[8], **Susan Groshen**[8], **Fabio Penna**[9], **Patrizio Odetti**[10], **Laura Perin**[2], **Peter S. Conti**[4], **Yuji Ikeno**[11], **Brian K. Kennedy**[12], **Pinchas Cohen**[1], **Todd E. Morgan**[1], **Tanya B. Dorff**[13], and **Valter D. Longo**[1,14,*]

[1]Longevity Institute, School of Gerontology, and Department of Biological Sciences, University of Southern California, Los Angeles, CA, USA

[2]GOFARR Laboratory, Children's Hospital Los Angeles, Division of Urology, Saban Research Institute, University of Southern California, Los Angeles, CA, USA

[3]Department of Pathology, Keck School of Medicine, University of Southern California, Los Angeles, CA, USA

[4]Molecular Imaging Center, Department of Radiology, Keck School of Medicine, University of Southern California, Los Angeles, CA, USA

[5]Institute for Liver and Digestive Health, Division of Medicine, University College London, Royal Free Hospital, London NW3 2PF, UK

[6]Department of Pathobiology and Medical Biotechnology, University of Palermo, Palermo, Italy

[7]Global Medicine Program, Keck School of Medicine, University of Southern California, Los Angeles, CA, USA

[8]Department of Preventive Medicine, Keck School of Medicine, University of Southern California, Los Angeles, CA, USA

[*]Correspondence should be addressed to Valter Longo at: Longevity Institute, Davis School of Gerontology and Dept. of Biological Sciences, University of Southern California, 3715 McClintock Avenue, Los Angeles, CA 90089-0191. vlongo@usc.edu.

[†]These authors contributed equally to this work.

Author Contribution

Preclinical studies: S.B., I.C., collected and alanlyzed the data. H.M., and M.G.M. performed the yeast experiments. G.N. and C.W.C. collected and processed the CBC data. C.W.C. performed FACS analysis. S.S. performed creatinine, BUN, ALT and renal histology. L.D. performed autopsies and histology. L.P.Y. and R.P. performed X-ray computed tomography. L.P.Y., R.P. and M.V. performed echocardiography. S.D.B. performed cytokine assay. F.P. performed protein expression for autophagy and myogenesis. L.J. and S.G. performed bioinformatic analyses. P.O., L.P., P.S.C., Y.I., B.K.K. and P.C. were involved in study design. S.B., T.E.M and V.D.L. designed the mouse study. *Clinical Trial:* V.D.L and M.W. designed the clinical trial, M.W. and T.D. supervised the clinical trial and performed data analysis together with S.B and H.M.. S.B., I.C. and V.D.L. wrote the paper. S.B. and I.C. contributed equally to this work. All authors discussed the results and commented on the manuscript.

Author information VDL and TEM have equity interest in L-Nutra, a company that develops medical food. Neither author had any role in data analysis.

[9]Department of Clinical and Biological Sciences, University of Torino, Torino, Italy

[10]Department of Internal Medicine, University of Genova, Genova, Italy

[11]Department of Pathology, Barshop Institute, University of Texas Health Science Center, San Antonio, TX, USA

[12]Buck Institute for Research on Aging, Novato, CA, USA

[13]Norris Comprehensive Cancer Center, Keck School of Medicine, University of Southern California, Los Angeles, CA, USA

[14]IFOM, FIRC Institute of Molecular Oncology, Milano, Italy

Summary

Prolonged fasting (PF) promotes stress resistance but its effects on longevity are poorly understood. We show that alternating PF and nutrient-rich medium extended yeast lifespan independently of established pro-longevity genes. In mice, four days of a diet that mimics fasting (FMD), developed to minimize the burden of PF, decreased the size of multiple organs/systems; an effect followed upon re-feeding by an elevated number of progenitor and stem cells and regeneration. Bi-monthly FMD cycles started at middle age extended longevity, lowered visceral fat, reduced cancer incidence and skin lesions, rejuvenated the immune system, and retarded bone mineral density loss. In old mice, FMD cycles promoted hippocampal neurogenesis, lowered IGF-1 levels and PKA activity, elevated NeuroD1, and improved cognitive performance. In a pilot clinical trial, three FMD cycles decreased risk factors/biomarkers for aging, diabetes, cardiovascular disease and cancer without major adverse effects, providing support for the use of FMDs to promote healthspan.

Introduction

Dietary composition and calorie level are key factors affecting aging and age-related diseases (Antosh et al., 2011; Blagosklonny et al., 2009; Fontana et al., 2010; Gems and Partridge, 2012; Lopez-Otin et al., 2013; Tatar et al., 2003). Dietary Restriction (DR) promotes metabolic and cellular changes that affect oxidative damage and inflammation, optimize energy metabolism, and enhance cellular protection (Haigis and Yankner, 2010; Johnson et al., 2000; Lee et al., 2012b; Longo and Finch, 2003; Mair and Dillin, 2008; Narasimhan et al., 2009; Smith et al., 2008). Fasting, the most extreme form of DR, which entails the abstinence from all food but not water, can be applied in a chronic manner as intermittent fasting (IF) or periodically as cycles of prolonged fasting (PF) lasting 2 or more days (Longo and Mattson, 2014). In rodents, IF promotes protection against diabetes, cancer, heart disease and neuro-degeneration (Longo and Mattson, 2014). In humans, IF and less severe regimens (e.g. consumption of approximately 500 kcal/day for 2 days a week), have beneficial effects on insulin, glucose, C-reactive protein, and blood pressure (Harvie et al., 2011).

PF cycles lasting 2 or more days but separated by at least a week of a normal diet are emerging as a highly effective strategy to protect normal cells and organs from a variety of toxins and toxic conditions (Raffaghello et al., 2008; Verweij et al., 2011) while increasing

the death of many cancer cell types (Lee et al., 2012a; Shi et al., 2012). PF causes a decrease in blood glucose, insulin and insulin-like growth factor I (IGF-I) (Lee et al., 2010) and is accompanied by autophagy (Cuervo et al., 2005; Madeo et al., 2010). Recently we have shown that PF causes a major reduction in the levels of white blood cells followed by stem-cell based immune system regeneration upon refeeding (Cheng et al., 2014). Others have reported on the role of PF in causing major decreases in liver and body mass in rats (Wasselin et al., 2014). However, prolonged water only fasting is difficult for the great majority of the population and its extreme nature could cause adverse effects, which include the exacerbation of previous malnourishments and dysfunctions, particularly in old and frail subjects. These concerns point to the need for dietary interventions that induce PF-like effects while minimizing the risk of adverse effects and the burden of complete food restriction.

Here we identified a diet that mimics the effects of fasting (Fasting Mimicking Diet, FMD) on markers associated with the stress resistance caused by PF, including low levels of glucose and IGF-1, and high levels of ketone bodies and IGFBP-1 (Longo and Mattson, 2014). We tested the hypothesis that cycles of the FMD lasting 4 days followed by a standard *ad libitum* diet could promote healthspan in mice. Additionally, we tested the effects of three cycles of a similar FMD in a pilot randomized clinical study with 38 subjects, 19 of whom were assigned to the FMD group.

Results and Discussion

Periodic Fasting in *S. cerevisiae* extends Lifespan and induces Stress Resistance

To determine whether the benefits of periodic starvation can be achieved in a simple organism, we tested the effects of cycles of prolonged fasting (PF) in *S. cerevisiae*. PF was implemented by switching wild type yeast cells back and forth from nutrient-rich medium to water every 48 hours. This period was selected to match the length of fasting shown to be effective in mice, but also to allow cells to undergo at least 4 cycles of PF before death. PF cycles extended both medium and maximum longevity (Fig 1 A, B) and increased the number of yeast cells survive hydrogen peroxide treatment by more than 100-fold (Fig 1 C). Surprisingly, the deletion of the serine threonine kinase Rim15, or of its downstream stress response transcription factors Msn2/4 and Gis1, well-established to be important or essential for longevity extension by genetic and dietary interventions (Fabrizio et al., 2001; Wei et al., 2008), did not prevent the lifespan effects of PF (Fig. 1 A, B). These results indicate that PF can protect simple organisms from both toxins and aging by mechanisms that are in part independent of conserved pro-longevity transcription factors, in agreement with findings in *C. elegans* that complete deprivation of food does not require the stress response transcription factor DAF-16, analogous to yeast Msn2/4 and Gis1 (Greer and Brunet, 2009; Kaeberlein et al., 2006).

Periodic FMD in aged mice

Periodic FMD without an overall reduction in calorie intake promotes visceral fat loss—We developed a very low calorie/low protein fasting-mimicking diet (FMD) that causes changes in markers associated with stress resistance or longevity (IGF-1, IGFBP-1,

ketone bodies, and glucose) that are similar to those caused by fasting (Table S1). Mice were fed the FMD starting at 16 months of age for 4 days twice a month and were fed an *ad lib* diet in the period between FMD cycles. Mice on the control diet reached maximum weight (36.6 ± 5.2g) at 21.5 months of age whereas those in the FMD group lost ~15% weight during each FMD cycle but regained most of the weight upon re-feeding (Fig. S1 A). However, FMD group mice maintained a similar weight between 16 and 22 months and then gradually lost weight (Fig. 1 D). Although FMD group mice were severely calorically restricted during the diet, they compensated for this restriction by overeating during the *ad lib* period, resulting in a 14 day cumulative calorie intake equivalent for the FMD and the *ad lib* groups (Fig. 1 E and Fig. S1 B). The average caloric intake in both cohorts increased after 25 months (Fig. 1 E).

At the end of the FMD and before re-feeding, blood glucose levels were 40% lower than those in the control diet group. Throughout the study, glucose returned to normal levels within 7 days of re-feeding (Fig. S1 C). Ketone bodies increased ~9-fold by the end of the FMD but returned to normal levels after re-feeding (Fig. S1 D). Serum insulin levels were reduced 10-fold after 4 days of the FMD and returned to baseline levels after re-feeding (Fig. S1 E). Reduced signaling of the growth hormone/IGF-I axis extends health-and lifespan in rodents (Brown-Borg, 2009; Guarente and Kenyon, 2000; Harrison et al., 2009; Junnila et al., 2013; Wullschleger et al., 2006). IGF-I was reduced by ~45% by the end of the FMD period but returned to normal levels, even after multiple FMD cycles (Fig. S1 F). IGFBP-1, which inhibits IGF-I, increased 8-fold by the end of the FMD regimen but its concentration returned to levels similar to those for *ad lib* mice within one week of re-feeding (Fig. S1 G).

To investigate diet-induced body composition changes, we evaluated lean body mass and body fat localization by microCT. At 28 months, FMD group mice had a trend ($p= 0.06$) for reduced total adipose tissue measured during the *ad lib* diet period between cycles (Fig. 1 F). Although subcutaneous adipose tissue volume (Fig. 1 G and Fig. 1 J, K; gray area) was not affected, visceral fat deposits (Fig. 1 H and Fig. 1 J, K; red area) were reduced in the FMD group compared to control group mice ($p < 0.05$). Lean body mass remained similar in the two groups (Fig. 1 I). These results indicate that FMD cycles can have profound effects on glucose and IGF-1 levels, but in mice these changes are reversed by the return to the *ad lib* diet.

Reduced organ size and regeneration—FMD (20.5 month), FMD-RF (7 days after resuming the *ad lib* diet post FMD; 20.5 month) and *ad lib* fed (16 and 20.5 month) mice were euthanized and organ weights measured. At the end of the FMD, we observed a reduction in organ weight in kidneys, heart, and liver (Fig. 1 L – N), but not in the lungs, spleen and brain (Fig. S1L – M), and a reduction in body weight (Fig. S1 H – J). The weights of these organs returned to pre-FMD levels after re-feeding.

The chronic use of bi-weekly FMD cycles caused no differences in systolic and diastolic left ventricular volume, ejection fraction and left ventricular mass, as measures for cardiac function in 25 month-old mice (Fig. S1 N- Q). Serum alanine transaminase, a liver atrophy marker, increased at the end of the FMD but returned to control levels upon re-feeding (Fig.

S1 R). Following re-feeding, liver cells repopulated in proximity to the hepatic blood vessels (Fig. 1 O 4, arrow). The effect of the FMD on hepatic regeneration 24h post re-feeding was supported by a 10-fold induction of a marker for hepatic cellular proliferation ($Ki67^+$) which is absent in G_0 cells (Fig. 1 P, Fig. S1 S). $Ki67^+$ remained elevated for at least 3 days post FMD. Renal function, assessed by serum creatinine and blood urea nitrogen measurements, revealed no alterations (Fig. S1 T – U) (Schnell et al., 2002). Renal histology, to evaluate glomerular and interstitial fibrosis, also showed no change in the number of sclerotic glomeruli (Fig. S1 V). These data are supportive of hepatic regeneration as a consequence of FMD-re-feeding cycles and with the lack of either liver or kidney toxicity even after 4 months on the FMD.

Postnatal growth and regeneration of the skeletal muscle requires myogenic precursors termed satellite cells (Sinha et al., 2014). Pax7 expression is critical for satellite cell biogenesis, survival, and self-renewal (Olguin et al., 2007) whereas the myogenic transcription factors MyoD and MyoG promote muscle development and differentiation (Perry and Rudnick, 2000). Pax7 up-regulation and reduced MyoD expression is observed in undifferentiated myogenic cells (Olguin et al., 2007). An age-dependent decline in Pax7 (Fig. 1 Q) and MyoD (and less pronounced in MyoG) was detected in 20 month-old mice (Fig. S1 W, X). At the end of the FMD, Pax7 expression was reduced by ~40% compared to that in control animals. A similar trend was also observed for MyoG ($p= 0.074$). One week after re-feeding, Pax7 expression in 20 month-old FMD group animals reached levels similar to those in 12 month old *ad lib* fed animals (Fig. 1 Q). By contrast, MyoD expression in old animals was not altered by the FMD (Fig. S1 W, X). Taken together these changes are consistent with muscle regeneration upon re-feeding although further analyses similar to those performed for the hematopoietic and nervous systems (*see below*) are necessary to confirm this hypothesis and determine the mechanisms responsible for it. Heterochronic parabiosis has been shown to increase the proliferative index of aged hepatocytes, as well as the proliferative and regenerative capacity of aged muscle satellite cells and to promote adult neurogenesis in an age-dependent fashion in mice (Conboy and Rando, 2012; Villeda et al., 2011). One of the proteins which has been implicated in muscle and brain regeneration and which may contribute to these regenerative effects in multiple systems is GDF11 (Katsimpardi et al., 2014; Sinha et al., 2014). It will be interesting to determine if part of the rejuvenating effect of the FMD may involve factors including or related to GDF11.

The failure to induce autophagy contributes to cellular damage, carcinogenesis and aging (Cuervo et al., 2005). Autophagy is mediated by several proteins that can be monitored by indirectly measuring autophagic sequestration (LC3) and degradation (p62) (Moscat and Diaz-Meco, 2011) (Fig. S1 Y, Z). p62 is consistently increased in autophagy deficient cells (Komatsu et al., 2007). An age-dependent increase in muscle p62 was observed in 20 month-old mice from the *ad lib* but not FMD group (Fig. 1 R), indicating that the FMD and possibly the associated regeneration protects muscle cells from age-dependent functional decline including the ability to maintain normal expression of autophagy proteins.

Tissue mineral density in both femora decreased in 28 months-old C57BL/6 mice compared to that in 12 months-old mice (Fig. 1 S) in agreement with previously published data (Shen et al., 2011). At 28 months, femoral bone density was higher in the FMD group compared to

that in the control diet group (Fig. 1 S), indicating that FMD cycles either attenuated age-dependent bone mineral density loss or induced bone regeneration.

Cancer and inflammation—C57BL/6 mice are prone to hematopoietic tumors, and mainly malignant lymphomas (Blackwell et al., 1995). Subcutaneous and internal masses caused by neoplasia, abscesses or both, were detected in aging mice (Fig. 2 A–H and Fig. S2 A – D). Necropsies indicated a 45% reduction in neoplasia incidence in the FMD group compared to that in the control group (Fig. 2 I). By the end of life, lymphomas affected ~67% of control mice but only ~40% of mice in the FMD group (Fig. 2 J) although the FMD did not cause a shift in the type of neoplasms. Notably, the FMD also postponed the occurrence of neoplasm-related deaths by over 3 months from 25.3 ± 0.66 months in the controls to 28.8 ± 0.72 months of age in the FMD cohort ($p= 0.003$) (Fig. 2 K). Furthermore, necropsies revealed that the number of animals with multiple (3 or more) abnormal lesions was more than 3-fold higher in the control than in the FMD group ($p= 0.0067$; Fishers exact test) (Fig. 2 L). Therefore, the cycles of the FMD started at middle age reduced tumor incidence, delayed their onset and caused a major reduction in the number of lesions, which may reflect a general switch from malignant to benign tumors.

Inflammation can play a key role in the development of many age-related diseases including cancer (Bartke et al., 2013; Morgan et al., 2007). Pathological analysis showed a reduced number of tissues with inflammation (e.g. reactive lymph nodes or chronic hepatic inflammation, Table S2) in the FMD mice compared to those in the control group (Fig. 2 M). One of the inflammatory conditions observed in C57BL/6 mice is severe ulcerating dermatitis (Fig. 2 N). Control animals had a ~20% incidence of progressing skin lesions that required animal sacrifice in contrast to ~10% for mice in the FMD fed group. These results indicate that the FMD protects against inflammation and inflammation-associated skin lesions (Coppe et al., 2010).

Effects of the FMD on immunosenescence and bone-marrow derived stem and progenitor cells—The age-linked decline in hematopoiesis causes a diminished or altered production of adaptive immune cells, a phenomenon known as “immunosenescence”, manifested as a shift in the lymphoid to myeloid ratio and elevated incidence of anemia and myeloid malignancies (Fig. 2 O – S) (Muller-Sieburg et al., 2004; Shaw et al., 2010). Complete blood counts indicated that the FMD causes a rejuvenation of the blood-profile (Fig. 2 O – S; Fig. S2 E – R) and a reversal of the age-dependent decline in the lymphoid to myeloid ratio (L/M) (Fig. 2 P), as well as of the age-dependent decline in platelets, and hemoglobin (Fig. 2 Q – S). Also, 4 months of FMD cycles resulted in an increase in red blood cell count and hemoglobin levels compared to baseline (Fig. 2 Q – S). We also measured a panel of 23 cytokines but did not detect changes except for elevated IL-12, and RANTES, as well as reduced GM-CSF in the FMD group (Fig. S2 S – U). These results indicate that chronic use of the FMD promotes immune system regeneration and rejuvenation, in agreement with our previous results on the effect of fasting on lymphocyte number (Cheng et al., 2014).

Among the bone marrow derived stem cells, hematopoietic stem cells and mesenchymal stem cells represent a potential source for adult tissue and organ regeneration. To investigate

whether the rejuvenating effects of the FMD may involve stem cells, we measured hematopoietic- (HSPC, $lin^{-}Scal\text{-}1^{+}C\text{-}kit^{+}CD45^{+}$) and mesenchymal- (MSPC, $lin^{-}Scal\text{-}1^{+}CD45^{-}$) stem and progenitor cells in the bone marrow. The number of HSPCs is known to increase with age, possibly to compensate for the reduction in function (Geiger and Van Zant, 2002; Morrison et al., 1996). This age-dependent increase may mask the effects of fasting or FMD in promoting stem-cell self-renewal, which we have recently shown for younger mice (Fig. S2 V) (Cheng et al., 2014). Unlike that of HSPCs, the number of MSPCs declines with aging (Bellantuono et al., 2009; Kasper et al., 2009). We confirmed this age-dependent decline comparing MSPCs number in mature (8- 10 months) and 20.5 months-old mice (Fig. 2 T) in agreement with previous reports (Kasper et al., 2009; Ratajczak et al., 2008). Remarkably, the number of MSPCs increased 5-fold in the FMD cohort (469.8± 179.5 FMD *vs*. 95.5± 16.7 CTRL; Fig. 2 T and Fig. S2 W) and that of $BrdU^{+}$ MSPC increased by 45-fold in FMD-treated mice (69.8± 34.0 FMD *vs*. 1.5± 0.6 CTRL) (Fig. 2 T and S2 X). Taken together, these data suggest that cycles of FMD are effective in promoting increases in hematopoietic and mesenchymal stem and progenitor cells which are likely to contribute to the regeneration of various cell types/systems.

Effects of the FMD on motor coordination, memory and neurogenesis—Aging is associated with the decline in locomotor and cognitive function (Lynch, 2004). To evaluate motor coordination and balance, we tested mouse performances on the accelerating rotarod (Shiotsuki et al., 2010). 23 month-old mice fed the FMD every 2 weeks (FMD-RF, tested one week after resuming the normal diet) were able to stay longer on the rotarod than mice in the control diet group (Fig. 3 A). We also assessed motor learning ability by examining performance improvement during subsequent trials. The mice from the FMD-RF group performed consistently better by staying on the accelerating rod longer than mice on the *ad lib* diet, although the rate of learning was similar in the two groups (sessions 2–5; Fig. 3 B). Mouse weight and best rotarod performance were associated (Pearson correlation coefficient $r= -0.46$; $p= 0.005$). When corrected for weight, rotarod performance was no longer significant ($p= 0.34$; data not shown), indicating that the FMD mice benefit from the fat loss).

To test the effect of the diet on cognitive performance we carried out working memory tests (Beninger et al., 1986) at 23 months of age (Fig. 3 C). Mice in the FMD cohort displayed enhanced spontaneous alternating behavior compared to control mice with no difference in the total number of arm entries (a measure of activity) (Fig. S3 A). Short-term cognitive performance and context-dependent memory were assessed with the novel object recognition test (Fig. 3 D, E) (Bernabeu et al., 1995). FMD-RF mice had a higher recognition index (RI= 0.60) compared to controls (RI= 0.52; $p< 0.01$) (Fig. 3 D). An increase in exploration time was observed for the FMD-RF mice for the new object, while the total exploration time remained the same (13.6 ± 0.9 CTRL *vs*. 13.4 ± 0.9 FMD-RF), suggesting enhanced short-term cognitive performance, not general activity (Fig. 3 E; Fig. S3 B).

As a measure of long-term memory, we measured spatial learning and memory using the Barnes Maze: a hippocampus-dependent cognitive task requiring spatial reference memory to locate a unique escape box by learning and memorizing visual clues (Fig. 3 F – K)

(Barnes, 1988). During the 7-day training period, FMD-RF mice performed better with regard to errors, deviation, latency and success rate compared to controls (Fig. 3 F – H). In the retention test, the FMD-RF group displayed better memory indicated by reduced deviation at day 14 (Fig. 3 G). Deviation of control diet mice at day 14 was similar to that at day 1, indicating that these mice did not remember the box location they had learned by day 7. Improvements in the search strategy, including the shifting from a random and serial search strategy to spatial strategies, were observed for the FMD but not the control diet group after day 3–4 (Fig. 3 J and K). Together, the behavioral tests suggests that FMD cycles improve motor learning and hippocampus-dependent short- and long-term memory in old animals.

Adult neurogenesis plays an important role in learning and memory (Clelland et al., 2009; Deng et al., 2010; Mattson, 2012). To determine whether the diet affected neurogenesis, we measured BrdU incorporation in the subgranular layer of control mice at the age of 8 weeks, 12 weeks, 6 months and 24 months (Fig. 4 B). Similarly to previously reported data, we observed an age-dependent decline in BrdU incorporation in the dentate gyrus (Lee et al., 2012c) (Fig. 4 B). To assess whether the cognitive improvements in the FMD group are associated with neural regeneration, we measured the proliferative index of DCX^+ immature neurons in the sub-granular cell layer of the dentate gyrus. $BrdU^+$ or $BrdU^+$ DCX^+ double-labeling indicated an increased proliferation of immature neurons in the FMD group compared to that in controls (Fig. 4 C–E). To investigate mechanisms of FMD induced neurogenesis, we fed 6 month-old mice, in which cellular proliferation in the dentate gyrus is reduced by more than 50% compared to that in 8 weeks-old mice (Fig. 4 B), with a single cycle of the FMD. After 72 hours on the FMD, we observed a reduction in circulating (Fig. S1 E) and hippocampal IGF-1 (Fig. 4 F) but increased IGF-1 receptor mRNA expression in the dentate gyrus region of the hippocampal formation (Fig. 4 G). Micro-dissected dentate gyrus-enriched samples from FMD mice displayed a major reduction in PKA activity (Fig. 4 H), and a 2-fold induction in the expression of NeuroD1 (Fig. 4 I); a transcription factor important for neuronal protection and differentiation (Gao et al., 2009). Similarly, a single cycle of the FMD increased radial glia-like cells (Type I) and non-radial precursor (Type II) neural stem cells (Fig. S4, B, C, F, G), immature neurons (Fig. S4 D, I – Q) and the dendrite covered area (Fig. S4 E, H) in CD-1 mice.

These results in two genetic backgrounds indicate that the FMD promotes neurogenesis in adult mice. Notably the brain did not undergo a measurable weight reduction during the FMD, indicating that regeneration can also occur independently of the organ size increase after refeeding. Thus, we hypothesize that alterations in circulating factors, such as the reduction in IGF-I levels and PKA signaling, can induce pro-regenerative changes that are both dependent and independent of the major cell proliferation that occurs during re-feeding, in agreement with our previous finding in bone marrow and blood cells (Cheng et al., 2014). Most likely, the increase in IGF-I and PKA after refeeding also contributes to the proliferative and regenerative process, raising the possibility that both low and high levels of these proteins can promote regeneration depending on the timing of their expression. Alternatively, the FMD may increase survival of newly-differentiated neurons, as observed in the dentate gyrus of alternate day-fed rodents (Lee et al., 2002; Mattson et al., 2001). The observed improvements in cognitive performance in the FMD cohort might be affected by

an the increase in neurogenesis mediated by PKA/CREB-dependent regulation of NeuroD1 (Cho et al., 2012; Sharma et al., 1999), which is known to increase neuronal survival and differentiation of hippocampal progenitors (Roybon et al., 2009), enhance functional integration of new neurons, and alleviate memory deficits in a mouse model of Alzheimer's disease (Richetin et al., 2015).

FMD and Lifespan—Control mice had a median lifespan of 25.5 months (Fig. 5 A), which was extended to 28.3 months (11% extension) in the FMD group ($p < 0.01$). The FMD showed an 18% extension effect at the 75% survival point, but only a 7.6% extension effect on the 25% survival point and no effect on maximum lifespan (Fig. 5 A, B), indicating that at very advanced ages the 4 day FMD may be beneficial for certain aspects and detrimental for others. Further analysis indicated that many deaths at very old ages occurred during or shortly (within 3 days) after completion of the FMD cycle (Fig. 5 E, *asterisk*). Based on this observation, at 26.5 months we shortened the FMD diet from 4 to 3 days and halted the FMD diet completely at 29.5 months. Analyses of the data indicates that whereas the shortening of the FMD from 4 to 3 days was associated with reduced mortality rates between 26.5 and 29.5 months, the halting of the FMD diet at 29.5 months did not reduce mortality further (Fig. 5 D). These results suggest that FMD cycles can have a potent effect on lifespan and healthspan but, at least for very old mice, a less severe (3 versus 4 days) low calorie and low protein diet may be preferable to continue to provide beneficial effects while minimizing malnourishment, in agreement with our recent work demonstrating opposite roles of high protein intake on health/mortality in mice and humans of middle to old and very old ages (Levine et al., 2014).

Periodic FMD in a Pilot Randomized Clinical Trial

Markers of aging and cell protection—To evaluate the feasibility and potential impact of a periodic low protein and low calorie FMD in humans, we conducted a pilot clinical trial in generally healthy adults. The components and levels of micro- and macro-nutrients in the human FMD were selected based on their ability to reduce IGF-I, increase IGFBP-1, reduce glucose, increase ketone bodies, and maximize nourishment (Fig. 6) in agreement with the FMD's effects in mice (Fig. S1). The development of the human diet took into account feasibility (e.g. high adherence to the dietary protocol) and therefore was designed to last 5 days every month and to provide between 34–54% of the normal caloric intake with a composition of at least 11–14% proteins, 42–43% carbohydrates and 44–46% fat. Subjects were randomized to either the FMD for 5 days every month for 3 months (3 cycles) or to a control group in which they continued to consume their normal diet (Fig. 6 A). Subjects were asked to resume their normal diet after the FMD period and were asked to not implement any changes in their dietary or exercise habits. 5 % of the subjects were disqualified due to non-compliance to the dietary protocol. 14 % of the enrolled subjects withdrew from the study due to non-diet related reasons (e.g. work- and travel-related scheduling issues). We present preliminary results of the pilot randomized clinical trial that includes a set of 19 participants who successfully completed 3 FMD cycles, as well as data for 19 participants who were randomized to continue on their normal diet and serve as controls. The control group included 9 female (47.4 %) and 10 male (52.6 %) of an average age of 35.4± 5.5 years and 38.0± 1.7 years, respectively. The FMD cohort included 7

females (36.8 %) and 12 males (63.2 %) of an average age of 41.8± 4.9 years and 42.5± 3.5 years, respectively (Fig. S5 A – B). The age range was 19.8 to 67.6 years for the control cohort and 27.6 to 70 years for the FMD cohort. The ethnicity was 58 % White, 18.5 % Hispanic, 18.5 % Asian and 5 % Black (Fig. S5 C). Subjects were evaluated by a baseline examination (Fig. 6 A). For the FMD group, the follow-up examinations occurred before resuming normal food intake at the end of the 1st FMD cycle (FMD) and after 5 to 8 days of normal dieting following the 3rd FMD cycle (FMD-RF, Fig. 6 A). The average time between the baseline and the FMD-RF assay/measurement points was 75.2± 2.7 days, whereas the time between baseline and the final examination was 74.5± 6.0 days in the control group. For all three FMD cycles, study participants self-reported adverse effects following Common Terminology Criteria for Adverse Events (Fig. S5 D). Adverse effects were higher after completion of the 1st FMD cycle compared to those during the 2nd and 3rd FMD cycles. However, the average reported severity of the side-effects was very low and below “mild” (<1 on a scale of 1 to 5).

In the FMD subjects, fasting blood glucose levels were reduced by 11.3 ± 2.3 % ($p < 0.001$; FMD) and remained 5.9 ± 2.1 % lower than baseline levels after resuming the normal diet following the third FMD cycle ($p < 0.05$; Fig. 6 B). Serum ketone bodies increased 3.7-fold at the end of the FMD regimen ($p < 0.001$) and returned to baseline levels following normal food intake (Fig. 6 C). Circulating IGF-I was reduced by ~24 % by the end of the FMD period ($p < 0.001$) and remained ~15 % lower after resuming the normal diet ($p < 0.01$; Fig. 6 D). IGFBP-1 was increased 1.5-fold at the end of the FMD regimen ($p < 0.01$) and returned to baseline levels following normal food intake (Fig. 6 E). These results indicate that the FMD group was highly complaint and generally did not consume foods not included in the FMD box provided to them.

Weight, abdominal fat, lean body mass and metabolic markers—In mice, the FMD caused weight loss and reduced visceral fat. We studied whether the FMD could have similar effects in humans by measuring body weight, abdominal fat, and lean body mass. The FMD resulted in a 3% reduction in body weight (3.1± 0.3 %; $p < 0.001$; Fig. 6 F) that remained lower at the completion of the study ($p < 0.01$; Fig. 6 F). Trunk fat percentage, measured by dual-energy X-ray absorptiometry, showed a trend ($p = 0.1$) for reduction after 3 FMD cycles and one week of normal dieting (Fig. 6 G), while the lean body mass adjusted for body weight was increased after completion of 3 cycles (Fig. 6 H), indicating that fat loss accounts for most of the weight loss. Pelvis bone mineral density was not affected by the FMD (Fig. S5 D).

A complete metabolic panel (Fig. S5 E – L) indicated no persistent metabolic changes due to the FMD except for lowered bilirubin and alkaline phosphatase following the return to the normal diet. Blood urea nitrogen, bilirubin, creatinine, alanine transaminase and aspartate transaminase showed changes immediately following the FMD, which remained within a safe physiological range. Together with the self-reported Common Terminology Criteria for Adverse Events, these results provide initial evidence that the periodic FMD is generally safe and causes fat loss without reducing lean body mass.

Cardiovascular Disease Risk Factors—In mice, the FMD caused a reduction in inflammation-associated diseases (Fig. 2). In humans, the serum level of C-reactive protein (CRP) is a marker of inflammation and risk factor for cardiovascular disease. At baseline, the average CRP level for the FMD subjects was 1.45± 0.4 mg/L (Fig. 6 I) and similar to the control group (1.29± 0.5 mg/L), indicating an average moderate risk for cardiovascular disease. CRP levels were reduced by the FMD cycles. 8 of the 19 FMD subjects had CRP levels in the moderate or high cardiovascular disease risk range (levels above 1.0 and 3 mg/L, respectively) at baseline. For 7 of them the levels returned to the normal range (levels below 1.0 mg/L), after 3 FMD cycles (Fig. 6 I). For the 11 participants with CRP levels below 1.0 mg/L at baseline, no changes were observed at the completion of the trial. These results indicate that periodic FMD cycles promote anti-inflammatory effects and reduce at least one risk factor for CVD.

Regenerative Markers—In mice, cycles of the FMD promoted an increase of mesenchymal stem- and progenitor cells (MSPC; Fig. 2). We therefore analyzed $lin^{-}CD184^{+}CD45^{-}$ MSPCs in the peripheral blood of human FMD subjects (Fig. 6 J). Although not significant, the percentage of MSPC in the peripheral blood mono-nucleated cell population showed a trend ($p= 0.1$) to increase from 0.15 ± 0.1 at baseline to 1.06 ± 0.6 at the end of FMD, with a subsequent return to baseline levels after re-feeding (0.27 ± 0.2). A larger randomized trial will be required to determine whether the number of specific populations of stem cells are in fact elevated by the FMD in humans.

In summary, this study indicates that FMD cycles induce long-lasting beneficial and/or rejuvenating effects on many tissues including those of the endocrine, immune, and nervous systems in mice and in markers for diseases and regeneration in humans. Although the clinical results will require confirmation by a larger randomized trial, the effects of FMD cycles on biomarkers/risk factors for aging, cancer, diabetes, and CVD, coupled with the very high compliance to the diet and its safety, indicate that this periodic dietary strategy has high potential to be effective in promoting human healthspan. Because prolonged FMDs such as the one tested here are potent and broad-spectrum, they should only be considered for use under medical supervision.

Material and Methods

Subjects

Experimental design and report was prepared following the CONSORT standards for randomized clinical trials where applicable. Available data from an ongoing pilot trial are presented. Subjects were recruited under protocols approved by the IRB (HS-12–00391) of the University of Southern California based on established inclusion (*generally healthy adult volunteers, 18–70 years of age, body mass index: 18.5 and up*) and exclusion (*any major medical condition and chronic diseases, mental illness, drug dependency, hormone replacement therapy (DHEA, estrogen, thyroid, testosterone), females who are pregnant or nursing, special dietary requirements or food allergies, alcohol dependency*) criteria. All participants signed informed consent forms and were not offered financial compensation for participation. Subjects were allocated (based on stratified sampling for age and gender) into

a control (N= 19) or experimental diet group (FMD, N= 19), followed by baseline examination. The control group continued normal food consumption and returned for a follow-up examination 3 months after enrollment. Subjects in the FMD cohort consumed the provided experimental diet consisting of 3 cycles of 5 continuous days of FMD followed by 25 days of normal food intake. During all three FMD cycles, study participants self-reported adverse effects following Common Terminology Criteria for Adverse Events. For the FMD group, follow-up examinations occurred before resuming normal food intake at the end of the 1st cycle (FMD) and also after 5 to 8 days of normal feeding following the end of the 3rd diet cycle (FMD-RF). Pre-specified outcome measures include adherence to the dietary protocol and evaluation of physiological markers during and after completion of the study. Examinations included height, dressed weight, body composition (including whole body fat, soft lean tissue, and bone mineral content) measured by dual energy x-ray absorptiometry (DEXA), and blood draw through venipuncture. All data was collected at the USC Diabetes & Obesity Research Institute. Complete metabolic panels were assayed by the Clinical Laboratories at the Keck Medical Center of USC immediately following blood draw. Data analysis was performed independent of study design. Complete data will be made available elsewhere upon completion of the study.

Human Diet

The human fasting mimicking diet (FMD) program is a plant-based diet program designed to attain fasting-like effects while providing micronutrient nourishment (vitamins, minerals etc.) to minimize the burden of fasting. It comprises proprietary vegetable-based soups, energy bars, energy drinks, chip snacks, chamomile flower tea, and a vegetable supplement formula tablet (Table S4). The human FMD diet consists of a 5 day regimen: day 1 diet of the diet supplies ~1090 kcal (10% protein, 56% fat, 34% carbohydrate), day 2–5 are identical in formulation and provide 725 kcal (9% protein, 44% fat, 47% carbohydrate).

Animals

All animal protocols were approved by the Institutional Animal Care and Use Committee (IACUC) of the University of Southern California. Experimental design and report was prepared following the ARRIVE standards for mouse work. 110 nine month old female C57Bl/6 (Charles River) retired breeders were maintained in a pathogen-free environment and housed in clear shoebox-cages in groups of three animals per cage with constant temperature and humidity and 12h/12h light-dark cycle and unlimited access to water. At 16 months of age, animals were randomly divided (by cage to avoid fighting) into the *ad lib* fed control (CTRL) group and the fasting mimicking diet (FMD) group. Bodyweight of individual animals was measured routinely every 2 weeks, prior to starting a new FMD cycle. N=9 mice were measured daily in the FMD and control cohort for safety evaluation and to establish a weight profile during the FMD cycle. Food intake was measured daily. Upon indication of progressing dermatitis, animals were treated with a triple antibiotic ointment (Fougera Pharmaceuticals Inc.) and were euthanized if the condition progressed. To reduce subjective bias, mice were randomly assigned (using the online Random Number Calculator from GraphPad) to any behavioral and physiological assessments shortly before any experiment. Mice that appeared weak and/or showed signs of illness were not included into any experiment. Upon death/sacrifice, autopsies were performed and all as abnormal

classified lesions submitted for evaluation by a pathologist. Autopsies were performed on 73 mice; 2 mice (one from each cohort respectively) were cannibalized and not available for autopsy. We also utilized strain-matched younger animals to establish age-dependent changes in risk factors using identical methods. In addition, 6 months old female CD-1 mice (Charles River) were used in supplemental experiments to measure adult neurogenesis.

Rodent Diets

Mice were fed *ad lib* with irradiated TD.7912 rodent chow (Harlan Teklad), containing 15.69 kJ/g of digestible energy (animal-based protein 3.92 kJ/g, carbohydrate 9.1 kJ/g, fat 2.67 kJ/g).

The FMD is based on a nutritional screen that identified ingredients which allow nourishment during periods of low calorie consumption (Brandhorst et al., 2013). The FMD consists of two different components designated as day 1 diet and day 2–4 diet that were fed in this order respectively. The day 1 diet consists of a mix of various low calorie broth powders, a vegetable medley powder, extra virgin olive oil, and essential fatty acids; day 2–4 diet consists of low calorie broth powders and glycerol. Both formulations were then substituted with hydrogel (Clear H2O) to achieve binding and to allow the supply of the food in the cage feeders. Day 1 diet contains 7.67 kJ/g (provided at ~50% of normal daily intake; protein 0.46 kJ/g, carbohydrate 2.2 kJ/g, fat 5.00 kJ/g), the day 2–4 diet is identical on all feeding days and contains 1.48 kJ/g (provided at ~10% of normal daily intake; protein/fat 0.01 kJ/g, carbohydrates 1.47 kJ/g). An alternative FMD containing 0.26 kJ/g (protein/fat 0.01 kJ/g, carbohydrates 0.25 kJ/g) was supplied for 3 days for the evaluation of adult neurogenesis. Mice consumed all the supplied food on each day of the FMD regimen and showed no signs of food aversion. At the end of either diet, we supplied TD.7912 chow *ad lib* for 10 days before starting another FMD cycle. Prior to the FMD, animals were transferred into fresh cages to avoid feeding on residual chow and coprophagy.

Survival analysis

The endpoint considered was survival defined as the duration in time between treatment starting date and date of death. Mice showing signs of severe stress, deteriorating health status or excess tumor load were designated as moribund and euthanized. Two mice in the FMD group were sacrificed due to seizure and head/neck injury, one mouse died during anesthesia. A total of 75 mice were included in the survival analysis, 46 in the control group and 29 in the FMD group. 12 were sacrificed due to progressing dermatitis (CTRL N=9, FMD N=3) and considered as deaths for the assessment of healthspan. Two cannibalized mice were considered as dead due to other reasons than neoplasia in the analysis. A secondary analysis that considered the 2 mice as dead because of neoplasia rendered similar results (data not shown).

Physiological Biomarkers

Prior to blood collection and glucose measurements, mice were withheld food for up to 4 hours to avoid interferences caused by food consumption. For mice, blood glucose was measured with the Precision Xtra blood glucose monitoring system (Abbott Laboratories).

An overview of all utilized commercial kits is given in the Supplemental Experimental Procedures.

Complete blood counts and Cytokines

Complete blood counts were performed using the Mindray BC-2800 VET auto hematology analyzer following the manufacturer's protocol. In brief, blood was collected from the tail vein in heparin-coated micro-hematocrit tubes. 20 μl of the heparinized blood was added to CDS diluent (Clinical Diagnostics Solution Inc.) and whole blood parameters were evaluated. Cytokines were measured using the Bio-Plex Cytokine Assay (Bio-Rad), following the manufacturers recommendation for serum analysis.

Echocardiography

Animals were anesthetized with 2% isoflurane, and the left hemithorax was shaved. The mice were placed on a temperature-controlled heating pad and heart rate was continuously monitored (400–550 bpm). Ultrasound trans-mission gel (Parker Laboratories Inc., Fairfield, NJ, USA) was used and the heart was imaged in the parasternal short-axis view. Two-dimensional B-mode images were obtained at the papillary muscle level using the high-resolution Vevo 770 Ultrasound system (VisualSonics) and analyzed using Vevo 770 V2.2.3 software (VisualSonics).

X-ray computed tomography (CT)-Scans

Mice (representing average body weight) were anesthetized using 2% inhalant isoflurane and placed in a fixed position on their back. Due to prolonged anesthesia times, animal number was kept at N=3 to minimize the risk of accidental death of old mice. Tissue bone mineral density (mg Hydroxyapatite/cm^3) of both femora was measured *in vivo* for N=5/group using the Siemens InveonCT scanner. Detailed description given in the Supplemental Experimental Procedures.

Bone marrow collection and FACS analysis

Bone marrow cells were harvested from femurs and tibia of mice in alpha-MEM media (Corning Cellgro). For mice, freshly collected bone marrow cells were washed with phosphate buffered saline (PBS) and stained with lineage-specific, Scal-1, c-Kit and BrdU antibodies (BD Biosciences) according to manufacturer's instructions. Analysis was performed using BD FACS diva on LSR II. Human $Lin^{-}CD184^{+}CD45^{-}$ mesenchymal stem/progenitor cells in the peripheral blood mono-nucleated cell population were identified using human hematopoietic lineage FITC cocktail, anti-human CD45 APC and anti-human CD184-PE (eBioscience, #22-7778-72, #17-9459-42, #12-9999-42).

Immunohistochemistry

For the detection of hematopoietic cell genesis, mice were injected intra-peritoneal with 2% filter-sterilized bromodeoxyuridine (BrdU; 10 mg/ml stock solution, Sigma) at a single dose of 200 mg/kg bodyweight in PBS 24 hours prior to the bone marrow collection. To analyze adult neurogenesis BrdU was injected at 50 mg/kg for 3 or 4 consecutive days (Fig. S 4)

prior to FMD feeding. Staining for BrdU, Ki67, Sox2, GFAP and doublecortin was performed as described in the Supplemental Experimental Procedures.

Western Blotting

A detailed description is given in the Supplemental Experimental Procedures.

Quantitative PCR

Relative transcript expression levels were measured by quantitative real-time PCR as described in the Supplemental Experimental Procedures.

Behavior Studies

A detailed description is given in the Supplemental Experimental Procedures. Y-maze 11 mice per treatment group were tested at 23 months of age. Spontaneous alternation behavior (SAB) score was calculated as the proportion of alternations (an arm choice differing from the previous two choices) to the total number of alternation opportunities. Accelerating rotarod At 23 months of age, 18 mice/group were evaluated using an accelerating rotarod. The speed and time after which the mice fell off were recorded. On two consecutive days, the mice were given three successive trials, for a total of six trials. Performance was measured with two variables: the mean of the individual best performance over the two consecutive trial days and the mean time the mice of each treatment group remained in balance over the six trial session as an index of training. Novel Object Recognition The testing session comprised two trials of 5 min of each. During the first trial (T1), the apparatus contained two identical objects. After a 1 hour delay interval, mice were placed back in the apparatus for the second trial (T2), now with one familiar and one new object. The time spent exploring each object during T1 and T2 were recorded manually. Recognition index was calculated as the time (in seconds) spent between familiar and new object. Barnes Maze 12 mice/group were tested twice daily for 7 days at 23 months of age. Success rate (100%, finding the escape box (EB) within 2 minutes or 0%, not finding the EB within 2 minutes), latency (time to enter the EB), number of errors (nose pokes and head deflections over false holes), deviation (how many holes away from the EB was the first error) and strategies used to locate the EB were recorded and averaged from two tests to obtain daily values. Search strategies were classified as random (crossings through the maze center), serial (searches in clockwise or counter-clockwise direction) or spatial (navigating directly to the EB with both error and deviation scores of no more than 3). Retention was assessed by testing once on day 14.

Yeast intermittent fasting

Yeast cells were streaked out from frozen stock onto YPD plates and incubated at 30°C for 2 days. Next, 3–5 colonies were inoculated in 2ml of liquid SDC and incubated overnight. 100μl of the over-night culture was added to 10ml of fresh SDC in a 50ml flask and incubated at 30°C for 3 days. On day 3, a dilution of the culture was plated on YPD plates to evaluate the number of viable cells. The remaining culture was spun down, media was removed and the pellet washed with sterile dH_2O twice before re-suspending in 10ml of sterile dH_2O in a 50ml flask followed by incubation for 2 days. On day 5, once again a

dilution of the culture was plated on YPD and the remainder was pelleted and re-suspended in 10ml of expired media followed by 48 hour incubation. This process was repeated by alternating dH_2O and expired media treatment every 2 days until the number of viable cells reached below 10% of the original culture.

To prepare expired media, 3–5 colonies were inoculated in 5ml of SDC overnight. 500μl of the overnight culture was added to 200ml SDC in a 500ml flask and incubated in an orbital shaker for 4 days. After the incubation period, the cultures were filtered using a 0.22micron filter and used for the duration of the experiment.

Statistical Analysis

All data are expressed as the mean ± SEM. For mice, all statistical analyses were two-sided and *P* values <0.05 were considered significant (* $p<0.05$, ** $p<0.01$, *** $p<0.001$). Differences among groups were tested either by Student *t*-test comparison, one-way ANOVA followed by Tukey's multiple comparison, or 2way ANOVA (for Barnes Maze) using GraphPad Prism v.5. Kaplan-Meier survival curves were compared using the Gehan-Breslow-Wilcoxon test. Competing risk analysis was performed to assess statistical differences in the rate of deaths. For human subjects statistical analysis was performed using the Wilcoxon signed-rank test and *P* values <0.05 were considered significant (* $p<0.05$, ** $p<0.01$, *** $p<0.001$).

Supplementary Material

Refer to Web version on PubMed Central for supplementary material.

Acknowledgements

We would like to thank Giusi Taormina, Shawna Chagoury and Lynn Baufeld for their assistance in the yeast chronological lifespan experiments. The Molecular Imaging Center at USC is supported in part by the National Center for Research Resources (NCRR, S10RR017964-01). National Institutes of Health (NIH); National Institutes of Aging (NIA) grants (AG20642, AG025135, AG034906); The Bakewell Foundation; The V Foundation for Cancer Research and a USC Norris Cancer Center pilot grant to VDL. The human study was funded by the USC Edna Jones chair fund. The funding sources had no involvement in study design; in the collection, analysis and interpretation of data; in the writing of the report; and in the decision to submit the article for publication. The content is solely the responsibility of the authors and does not necessarily represent the official views of the National Institute on Aging or the National Institutes of Health. The University of Southern California has licensed intellectual property to L-Nutra that is under study in this research. As part of this license agreement, the University has the potential to receive royalty payments from L-Nutra.

References

Antosh M, Whitaker R, Kroll A, Hosier S, Chang C, Bauer J, Cooper L, Neretti N, Helfand SL. Comparative transcriptional pathway bioinformatic analysis of dietary restriction, Sir2, p53 and resveratrol life span extension in Drosophila. Cell Cycle. 2011; 10:904–911. [PubMed: 21325893]

Barnes CA. Spatial learning and memory processes: the search for their neurobiological mechanisms in the rat. Trends Neurosci. 1988; 11:163–169. [PubMed: 2469185]

Bartke A, Sun LY, Longo V. Somatotropic signaling: trade-offs between growth, reproductive development, and longevity. Physiol Rev. 2013; 93:571–598. [PubMed: 23589828]

Bellantuono I, Aldahmash A, Kassem M. Aging of marrow stromal (skeletal) stem cells and their contribution to age-related bone loss. Biochimica et biophysica acta. 2009; 1792:364–370. [PubMed: 19419706]

Beninger RJ, Jhamandas K, Boegman RJ, el-Defrawy SR. Effects of scopolamine and unilateral lesions of the basal forebrain on T-maze spatial discrimination and alternation in rats. Pharmacol Biochem Behav. 1986; 24:1353–1360. [PubMed: 3725838]

Bernabeu R, de Stein ML, Fin C, Izquierdo I, Medina JH. Role of hippocampal NO in the acquisition and consolidation of inhibitory avoidance learning. Neuroreport. 1995; 6:1498–1500. [PubMed: 7579133]

Blackwell BN, Bucci TJ, Hart RW, Turturro A. Longevity, body weight, and neoplasia in ad libitum-fed and diet-restricted C57BL6 mice fed NIH-31 open formula diet. Toxicol Pathol. 1995; 23:570–582. [PubMed: 8578100]

Blagosklonny MV, Campisi J, Sinclair DA. Aging: past, present and future. Aging (Albany NY). 2009; 1:1–5. [PubMed: 20157590]

Brandhorst S, Wei M, Hwang S, Morgan TE, Longo VD. Short-term calorie and protein restriction provide partial protection from chemotoxicity but do not delay glioma progression. Exp Gerontol. 2013

Brown-Borg HM. Hormonal control of aging in rodents: the somatotropic axis. Molecular and cellular endocrinology. 2009; 299:64–71. [PubMed: 18674587]

Cheng C-W, Adams Gregor B, Perin L, Wei M, Zhou X, Lam Ben S, Da Sacco S, Mirisola M, Quinn David I, Dorff Tanya B, Kopchick John J, Longo Valter D. Prolonged Fasting Reduces IGF-1/PKA to Promote Hematopoietic-Stem-Cell-Based Regeneration and Reverse Immunosuppression. Cell Stem Cell. 2014; 14:810–823. [PubMed: 24905167]

Cho IS, Jung M, Kwon KS, Moon E, Cho JH, Yoon KH, Kim JW, Lee YD, Kim SS, Suh-Kim H. Deregulation of CREB signaling pathway induced by chronic hyperglycemia downregulates NeuroD transcription. PloS one. 2012; 7:e34860. [PubMed: 22509362]

Clelland CD, Choi M, Romberg C, Clemenson GD Jr, Fragniere A, Tyers P, Jessberger S, Saksida LM, Barker RA, Gage FH, Bussey TJ. A functional role for adult hippocampal neurogenesis in spatial pattern separation. Science. 2009; 325:210–213. [PubMed: 19590004]

Conboy IM, Rando TA. Heterochronic parabiosis for the study of the effects of aging on stem cells and their niches. Cell Cycle. 2012; 11:2260–2267. [PubMed: 22617385]

Coppe JP, Desprez PY, Krtolica A, Campisi J. The senescence-associated secretory phenotype: the dark side of tumor suppression. Annual review of pathology. 2010; 5:99–118.

Cuervo AM, Bergamini E, Brunk UT, Droge W, Ffrench M, Terman A. Autophagy and aging: the importance of maintaining “clean” cells. Autophagy. 2005; 1:131–140. [PubMed: 16874025]

Deng W, Aimone JB, Gage FH. New neurons and new memories: how does adult hippocampal neurogenesis affect learning and memory? Nat Rev Neurosci. 2010; 11:339–350. [PubMed: 20354534]

Fabrizio P, Pozza F, Pletcher SD, Gendron CM, Longo VD. Regulation of longevity and stress resistance by Sch9 in yeast. Science. 2001; 292:288–290. [PubMed: 11292860]

Fontana L, Partridge L, Longo VD. Extending healthy life span--from yeast to humans. Science. 2010; 328:321–326. [PubMed: 20395504]

Gao Z, Ure K, Ables JL, Lagace DC, Nave KA, Goebbels S, Eisch AJ, Hsieh J. Neurod1 is essential for the survival and maturation of adult-born neurons. Nature neuroscience. 2009; 12:1090–1092. [PubMed: 19701197]

Geiger H, Van Zant G. The aging of lympho-hematopoietic stem cells. Nature immunology. 2002; 3:329–333. [PubMed: 11919569]

Gems D, Partridge L. Genetics of longevity in model organisms: debates and paradigm shifts. Annu Rev Physiol. 2012; 75:621–644. [PubMed: 23190075]

Greer EL, Brunet A. Different dietary restriction regimens extend lifespan by both independent and overlapping genetic pathways in C. elegans. Aging cell. 2009; 8:113–127. [PubMed: 19239417]

Guarente L, Kenyon C. Genetic pathways that regulate ageing in model organisms. Nature. 2000; 408:255–262. [PubMed: 11089983]

Haigis MC, Yankner BA. The aging stress response. Mol Cell. 2010; 40:333–344. [PubMed: 20965426]

Harrison DE, Strong R, Sharp ZD, Nelson JF, Astle CM, Flurkey K, Nadon NL, Wilkinson JE, Frenkel K, Carter CS, Pahor M, Javors MA, Fernandez E, Miller RA. Rapamycin fed late in life extends lifespan in genetically heterogeneous mice. Nature. 2009; 460:392–395. [PubMed: 19587680]

Harvie MN, Pegington M, Mattson MP, Frystyk J, Dillon B, Evans G, Cuzick J, Jebb SA, Martin B, Cutler RG, Son TG, Maudsley S, Carlson OD, Egan JM, Flyvbjerg A, Howell A. The effects of intermittent or continuous energy restriction on weight loss and metabolic disease risk markers: a randomized trial in young overweight women. International journal of obesity. 2011; 35:714–727. [PubMed: 20921964]

Johnson TE, Cypser J, de Castro E, de Castro S, Henderson S, Murakami S, Rikke B, Tedesco P, Link C. Gerontogenes mediate health and longevity in nematodes through increasing resistance to environmental toxins and stressors. Exp Gerontol. 2000; 35:687–694. [PubMed: 11053658]

Junnila RK, List EO, Berryman DE, Murrey JW, Kopchick JJ. The GH/IGF-1 axis in ageing and longevity. Nature reviews. Endocrinology. 2013; 9:366–376. [PubMed: 23591370]

Kaeberlein TL, Smith ED, Tsuchiya M, Welton KL, Thomas JH, Fields S, Kennedy BK, Kaeberlein M. Lifespan extension in Caenorhabditis elegans by complete removal of food. Aging cell. 2006; 5:487–494. [PubMed: 17081160]

Kasper G, Mao L, Geissler S, Draycheva A, Trippens J, Kuhnisch J, Tschirschmann M, Kaspar K, Perka C, Duda GN, Klose J. Insights into mesenchymal stem cell aging: involvement of antioxidant defense and actin cytoskeleton. Stem Cells. 2009; 27:1288–1297. [PubMed: 19492299]

Katsimpardi L, Litterman NK, Schein PA, Miller CM, Loffredo FS, Wojtkiewicz GR, Chen JW, Lee RT, Wagers AJ, Rubin LL. Vascular and neurogenic rejuvenation of the aging mouse brain by young systemic factors. Science. 2014; 344:630–634. [PubMed: 24797482]

Komatsu M, Waguri S, Koike M, Sou YS, Ueno T, Hara T, Mizushima N, Iwata J, Ezaki J, Murata S, Hamazaki J, Nishito Y, Iemura S, Natsume T, Yanagawa T, Uwayama J, Warabi E, Yoshida H, Ishii T, Kobayashi A, Yamamoto M, Yue Z, Uchiyama Y, Kominami E, Tanaka K. Homeostatic levels of p62 control cytoplasmic inclusion body formation in autophagy-deficient mice. Cell. 2007; 131:1149–1163. [PubMed: 18083104]

Lee C, Raffaghello L, Brandhorst S, Safdie FM, Bianchi G, Martin-Montalvo A, Pistoia V, Wei M, Hwang S, Merlino A, Emionite L, de Cabo R, Longo VD. Fasting Cycles Retard Growth of Tumors and Sensitize a Range of Cancer Cell Types to Chemotherapy. Sci Transl Med. 2012a

Lee C, Raffaghello L, Longo VD. Starvation, detoxification, and multidrug resistance in cancer therapy. Drug Resist Updat. 2012b; 15:114–122. [PubMed: 22391012]

Lee C, Safdie FM, Raffaghello L, Wei M, Madia F, Parrella E, Hwang D, Cohen P, Bianchi G, Longo VD. Reduced levels of IGF-I mediate differential protection of normal and cancer cells in response to fasting and improve chemotherapeutic index. Cancer research. 2010; 70:1564–1572. [PubMed: 20145127]

Lee J, Duan W, Mattson MP. Evidence that brain-derived neurotrophic factor is required for basal neurogenesis and mediates, in part, the enhancement of neurogenesis by dietary restriction in the hippocampus of adult mice. J Neurochem. 2002; 82:1367–1375. [PubMed: 12354284]

Lee SW, Clemenson GD, Gage FH. New neurons in an aged brain. Behavioural brain research. 2012c; 227:497–507. [PubMed: 22024433]

Levine ME, Suarez JA, Brandhorst S, Balasubramanian P, Cheng CW, Madia F, Fontana L, Mirisola MG, Guevara-Aguirre J, Wan J, Passarino G, Kennedy BK, Wei M, Cohen P, Crimmins EM, Longo VD. Low protein intake is associated with a major reduction in IGF-1, cancer, and overall mortality in the 65 and younger but not older population. Cell metabolism. 2014; 19:407–417. [PubMed: 24606898]

Longo VD, Finch CE. Evolutionary medicine: from dwarf model systems to healthy centenarians? Science. 2003; 299:1342–1346. [PubMed: 12610293]

Longo VD, Mattson MP. Fasting: Molecular Mechanisms and Clinical Applications. Cell metabolism. 2014; 19:181–192. [PubMed: 24440038]

Lopez-Otin C, Blasco MA, Partridge L, Serrano M, Kroemer G. The hallmarks of aging. Cell. 2013; 153:1194–1217. [PubMed: 23746838]

Lynch MA. Long-term potentiation and memory. Physiol Rev. 2004; 84:87–136. [PubMed: 14715912]

Madeo F, Tavernarakis N, Kroemer G. Can autophagy promote longevity? Nature cell biology. 2010; 12:842–846. [PubMed: 20811357]

Mair W, Dillin A. Aging and survival: the genetics of life span extension by dietary restriction. Annu Rev Biochem. 2008; 77:727–754. [PubMed: 18373439]

Mattson MP. Energy intake and exercise as determinants of brain health and vulnerability to injury and disease. Cell metabolism. 2012; 16:706–722. [PubMed: 23168220]

Mattson MP, Duan W, Lee J, Guo Z. Suppression of brain aging and neurodegenerative disorders by dietary restriction and environmental enrichment: molecular mechanisms. Mechanisms of ageing and development. 2001; 122:757–778. [PubMed: 11322996]

Morgan TE, Wong AM, Finch CE. Anti-inflammatory mechanisms of dietary restriction in slowing aging processes. Interdiscip Top Gerontol. 2007; 35:83–97. [PubMed: 17063034]

Morrison SJ, Wandycz AM, Akashi K, Globerson A, Weissman IL. The aging of hematopoietic stem cells. Nature medicine. 1996; 2:1011–1016.

Moscat J, Diaz-Meco MT. Feedback on fat: p62-mTORC1-autophagy connections. Cell. 2011; 147:724–727. [PubMed: 22078874]

Muller-Sieburg CE, Cho RH, Karlsson L, Huang JF, Sieburg HB. Myeloid-biased hematopoietic stem cells have extensive self-renewal capacity but generate diminished lymphoid progeny with impaired IL-7 responsiveness. Blood. 2004; 103:4111–4118. [PubMed: 14976059]

Narasimhan SD, Yen K, Tissenbaum HA. Converging pathways in lifespan regulation. Current biology : CB. 2009; 19:R657–R666. [PubMed: 19674551]

Olguin HC, Yang Z, Tapscott SJ, Olwin BB. Reciprocal inhibition between Pax7 and muscle regulatory factors modulates myogenic cell fate determination. The Journal of cell biology. 2007; 177:769–779. [PubMed: 17548510]

Perry RL, Rudnick MA. Molecular mechanisms regulating myogenic determination and differentiation. Frontiers in bioscience : a journal and virtual library. 2000; 5:D750–D767. [PubMed: 10966875]

Raffaghello L, Lee C, Safdie FM, Wei M, Madia F, Bianchi G, Longo VD. Starvation- dependent differential stress resistance protects normal but not cancer cells against high-dose chemotherapy. Proceedings of the National Academy of Sciences of the United States of America. 2008; 105:8215–8220. [PubMed: 18378900]

Ratajczak MZ, Zuba-Surma EK, Wysoczynski M, Ratajczak J, Kucia M. Very small embryonic-like stem cells: characterization, developmental origin, and biological significance. Exp Hematol. 2008; 36:742–751. [PubMed: 18474305]

Richetin K, Leclerc C, Toni N, Gallopin T, Pech S, Roybon L, Rampon C. Genetic manipulation of adult-born hippocampal neurons rescues memory in a mouse model of Alzheimer's disease. Brain : a journal of neurology. 2015; 138:440–455. [PubMed: 25518958]

Roybon L, Hjalt T, Stott S, Guillemot F, Li JY, Brundin P. Neurogenin2 directs granule neuroblast production and amplification while NeuroD1 specifies neuronal fate during hippocampal neurogenesis. PloS one. 2009; 4:e4779. [PubMed: 19274100]

Schnell MA, Hardy C, Hawley M, Propert KJ, Wilson JM. Effect of blood collection technique in mice on clinical pathology parameters. Hum Gene Ther. 2002; 13:155–161. [PubMed: 11779419]

Sharma A, Moore M, Marcora E, Lee JE, Qiu Y, Samaras S, Stein R. The NeuroD1/BETA2 sequences essential for insulin gene transcription colocalize with those necessary for neurogenesis and p300/CREB binding protein binding. Molecular and cellular biology. 1999; 19:704–713. [PubMed: 9858593]

Shaw AC, Joshi S, Greenwood H, Panda A, Lord JM. Aging of the innate immune system. Curr Opin Immunol. 2010; 22:507–513. [PubMed: 20667703]

Shen J, Tsai YT, Dimarco NM, Long MA, Sun X, Tang L. Transplantation of mesenchymal stem cells from young donors delays aging in mice. Sci Rep. 2011; 1:67. [PubMed: 22355586]

Shi Y, Felley-Bosco E, Marti TM, Orlowski K, Pruschy M, Stahel RA. Starvation- induced activation of ATM/Chk2/p53 signaling sensitizes cancer cells to cisplatin. BMC Cancer. 2012; 12:571. [PubMed: 23211021]

Shiotsuki H, Yoshimi K, Shimo Y, Funayama M, Takamatsu Y, Ikeda K, Takahashi R, Kitazawa S, Hattori N. A rotarod test for evaluation of motor skill learning. J Neurosci Methods. 2010; 189:180–185. [PubMed: 20359499]

Sinha M, Jang YC, Oh J, Khong D, Wu EY, Manohar R, Miller C, Regalado SG, Loffredo FS, Pancoast JR, Hirshman MF, Lebowitz J, Shadrach JL, Cerletti M, Kim MJ, Serwold T, Goodyear LJ, Rosner B, Lee RT, Wagers AJ. Restoring systemic GDF11 levels reverses age-related dysfunction in mouse skeletal muscle. Science. 2014; 344:649–652. [PubMed: 24797481]

Smith ED, Kaeberlein TL, Lydum BT, Sager J, Welton KL, Kennedy BK, Kaeberlein M. Age- and calorie-independent life span extension from dietary restriction by bacterial deprivation in Caenorhabditis elegans. BMC developmental biology. 2008; 8:49. [PubMed: 18457595]

Tatar M, Bartke A, Antebi A. The endocrine regulation of aging by insulin-like signals. Science. 2003; 299:1346–1351. [PubMed: 12610294]

Verweij M, van Ginhoven TM, Mitchell JR, Sluiter W, van den Engel S, Roest HP, Torabi E, Ijzermans JN, Hoeijmakers JH, de Bruin RW. Preoperative fasting protects mice against hepatic ischemia/reperfusion injury: mechanisms and effects on liver regeneration. Liver Transpl. 2011; 17:695–704. [PubMed: 21618690]

Villeda SA, Luo J, Mosher KI, Zou B, Britschgi M, Bieri G, Stan TM, Fainberg N, Ding Z, Eggel A, Lucin KM, Czirr E, Park JS, Couillard-Despres S, Aigner L, Li G, Peskind ER, Kaye JA, Quinn JF, Galasko DR, Xie XS, Rando TA, Wyss-Coray T. The ageing systemic milieu negatively regulates neurogenesis and cognitive function. Nature. 2011; 477:90–94. [PubMed: 21886162]

Wasselin T, Zahn S, Maho YL, Dorsselaer AV, Raclot T, Bertile F. Exacerbated oxidative stress in the fasting liver according to fuel partitioning. Proteomics. 2014; 14:1905–1921. [PubMed: 24920225]

Wei M, Fabrizio P, Hu J, Ge H, Cheng C, Li L, Longo VD. Life span extension by calorie restriction depends on Rim15 and transcription factors downstream of Ras/PKA, Tor, and Sch9. PLoS genetics. 2008; 4:e13. [PubMed: 18225956]

Wullschleger S, Loewith R, Hall MN. TOR signaling in growth and metabolism. Cell. 2006; 124:471–484. [PubMed: 16469695]

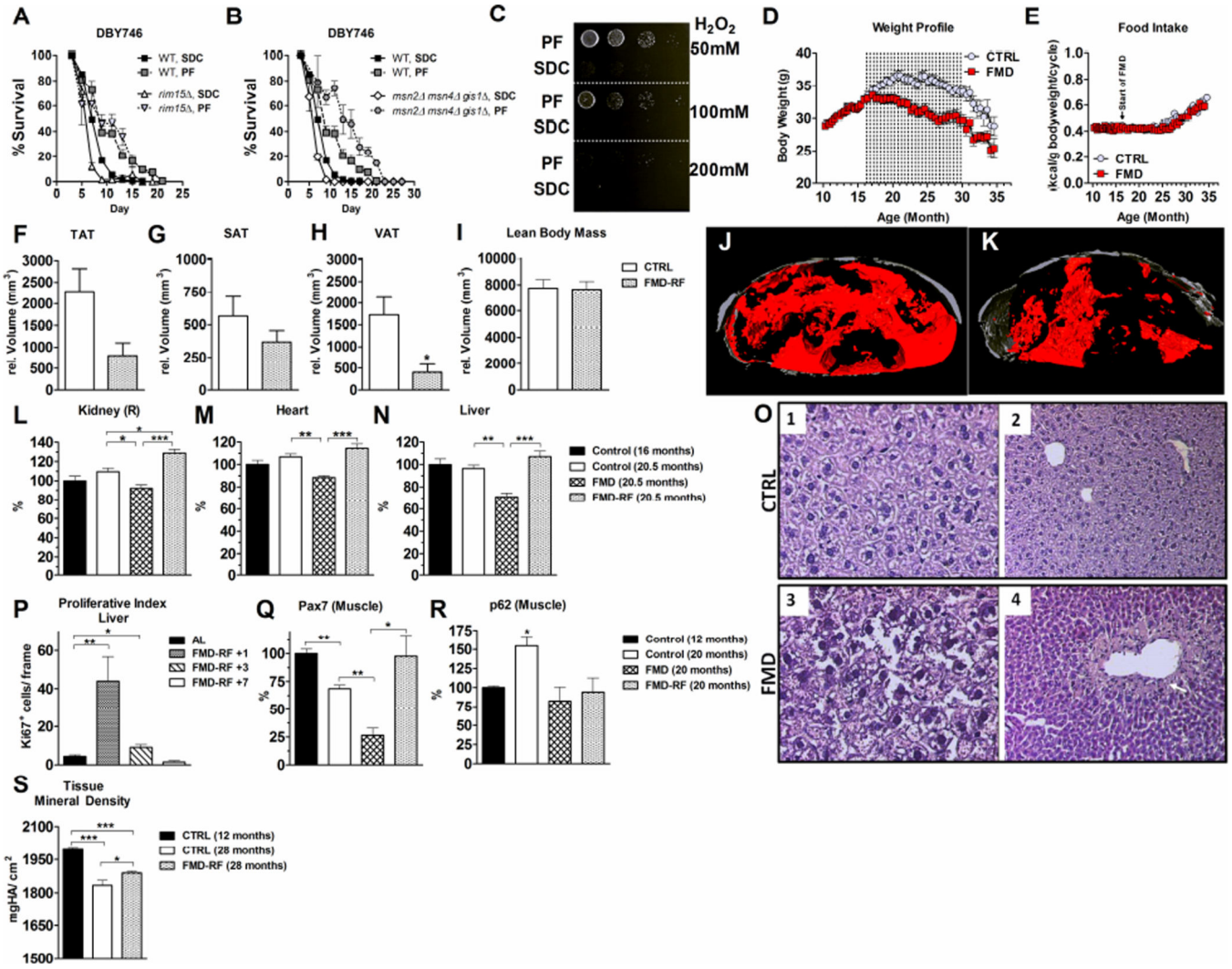

Figure 1. Periodic FMD promotes a lean bodyweight, improves health-span and promotes tissue regeneration

A) Periodic fasting (PF, alternating cycles of SDC media and water) prolongs lifespan in wild type (WT) *S. Cerevisiae* (DBY746), in *rim15*Δ and **B)***msn2*Δ *msn4*Δ *gis1*Δ DBY746 mutants. **C)** PF induces cellular stress resistance against hydrogen peroxide in *S. Cerevisiae* (DBY746). **D)** Mouse body weight profile. Dotted lines represent FMD cycles. **E)** Consumed kcal/g of bodyweight. **F)** Total adipose tissue (TAT), **G)** Subcutaneous adipose tissue (SAT), **H)** Visceral adipose tissue (VAT) and **I)** Lean body mass at 28 months of age. N= 3/group. **J) – K)** Representative images of the SAT (gray) and VAT (red) in the lumbar L3 region. **L)** Kidney **M)** Heart and **N)** Liver weight as % change. N= 8-10/group. **O)** Liver H&E staining of control (1, 2) and FMD mouse at the end of the FMD regimen (3) or 24 hours after re-feeding (4). Unorganized cells (*arrow*) indicate liver repopulation. 1, 3: 40X magnification; 2, 4: 20X magnification. **P)** Hepatic proliferative index ($Ki67^{+}$) after 1, 3 and 7 days of refeeding compared to control. N= 3-4/group. **Q)** Pax7 and **R)** p62 protein expression level, N= 3-4/group. **S)** Tissue mineral density (mg Hydroxyapatite/cm^3) of the femur. N= 5/group. All data are expressed as the mean ± SEM.

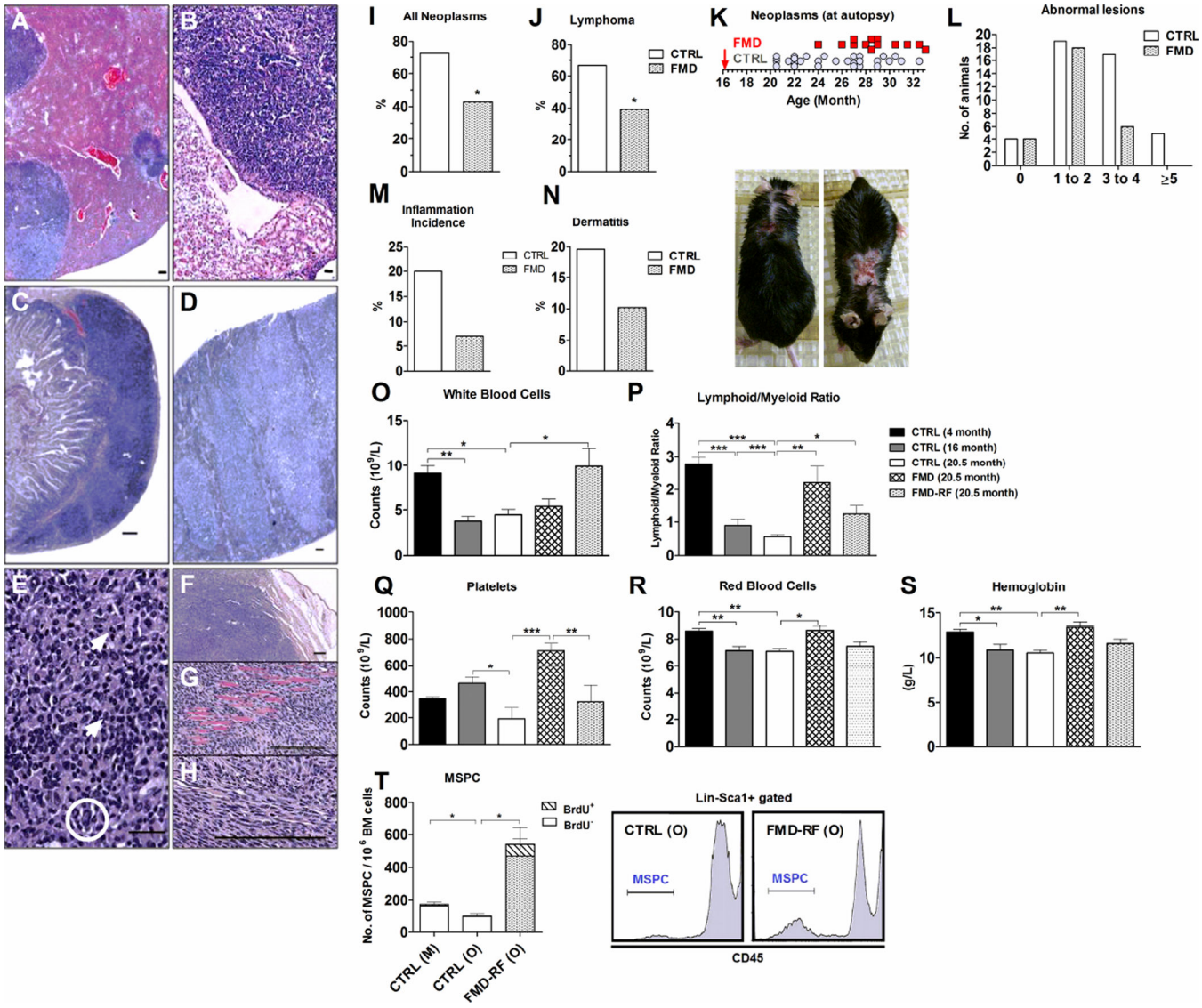

Figure 2. Periodic FMD cycle reduce and delay cancer, rejuvenate the hematopoietic system and induce mesenchymal stem/progenitor cells

A) Hepatic lymphomatous nodules (bar= 400 microns). **B)** Lymphoma in the renal medulla (bar= 100 microns), **C)** in a mesenteric lymph node (bar= 100 microns) and **D)** in the spleen (bar= 100 microns). **E)** Hepatic lymphoma containing atypical cells with abnormal DNA (*circle*) and mitosis (*arrows*, bar= 100 microns). Subcutaneous fibrosarcoma in relationship to **F)** the epidermis and with invasion into **G)** the skeletal muscle tissue. **H)** Cytological details (bar= 100 microns). **I)** Autopsy-confirmed neoplasms. **J)** Lymphoma incidence. **K)** Neoplasms in relationship to the onset (*arrow*) of the FMD diet. **L)** Number of animals with 0 to more than 5 abnormal lesions determined at autopsy. **M)** Inflammatory incidence. **N)** Dermatitis incidence in %. Images show progression of dermatitis. **O) – T)** Complete blood counts. N= 7-12/group. **O)** White blood cells, **P)** Lymphoid: myeloid ratio. **Q)** Platelets, **R)** Red blood cells and **S)** Hemoglobin. Other CBC parameters are summarized in Table S3 and Figure S8. **T)** $lin^{-}Scal\text{-}1^{+}CD45^{-}$ mesenchymal stem/progenitor cells (MSPC) in bone

marrow cells from control mature (M, 8–10 month), old (O, 20.5 month), and FMD mice 7 days after refeeding (FMD-RF; 20.5 month). N= 4-5/group. All data are expressed as the mean ± SEM.

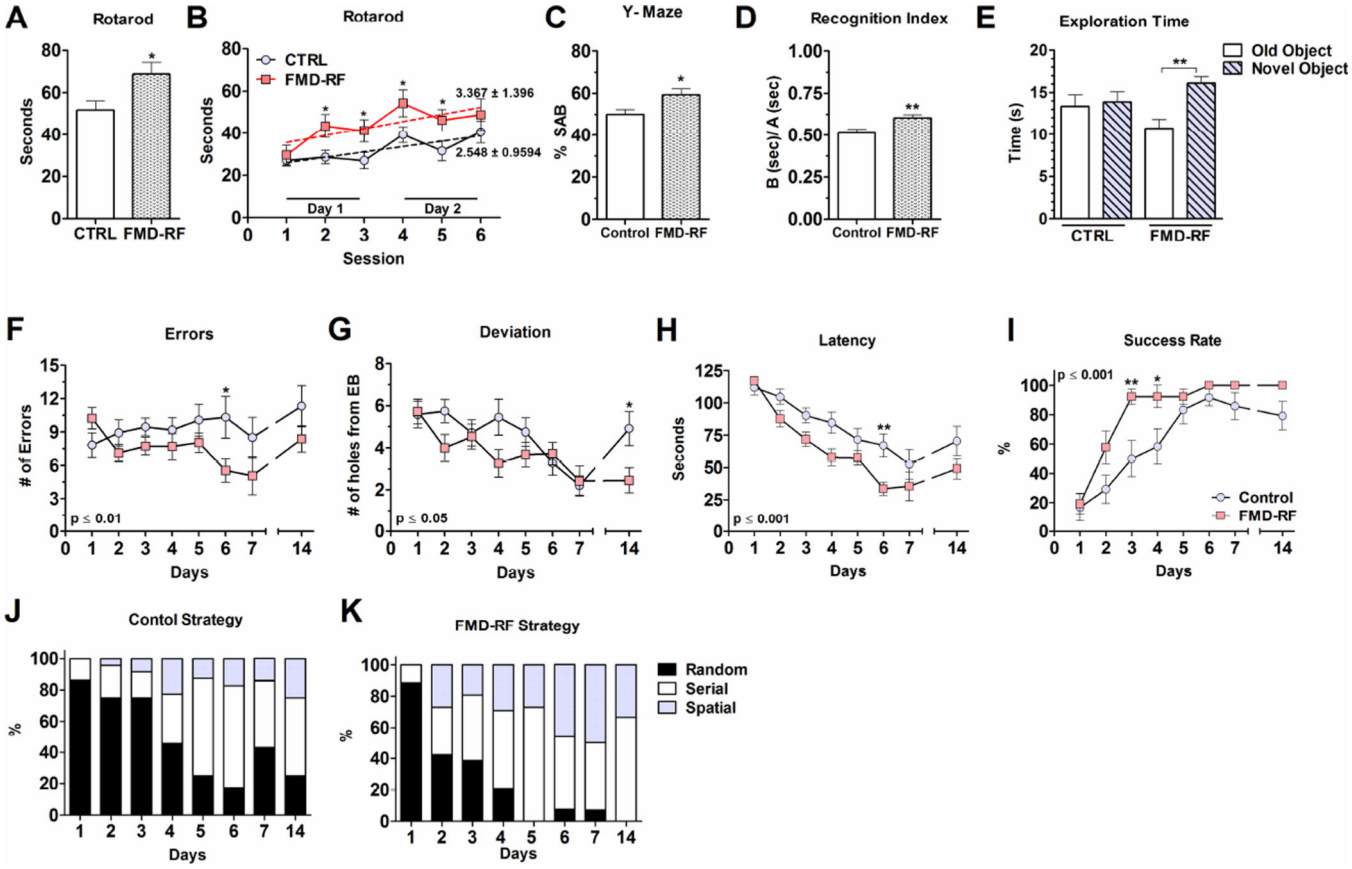

Figure 3. Periodic FMD cycle improve motor coordination, hippocampal dependent learning, short- and long-term memory

A) Best Rotarod performance score at 23 months. N= 18/group. **B)** Rotarod performance as linear regression for each cohort (dashed lines). N= 18/group. **C)** Spontaneous alternation behavior (SAB) at 23 months. N= 11/group. **D)** Recognition index at 23 months in the novel object recognition task. **E)** Exploration time of the old *vs*. novel object (New, dashed bar). N= 8/group. **F) – I)** Success rate, latency, error number and deviation from escape box in the Barnes maze at 23 months (N= 7-12/group). **J) – K)** Strategies used to locate escape box. All data are expressed as the mean ± SEM.

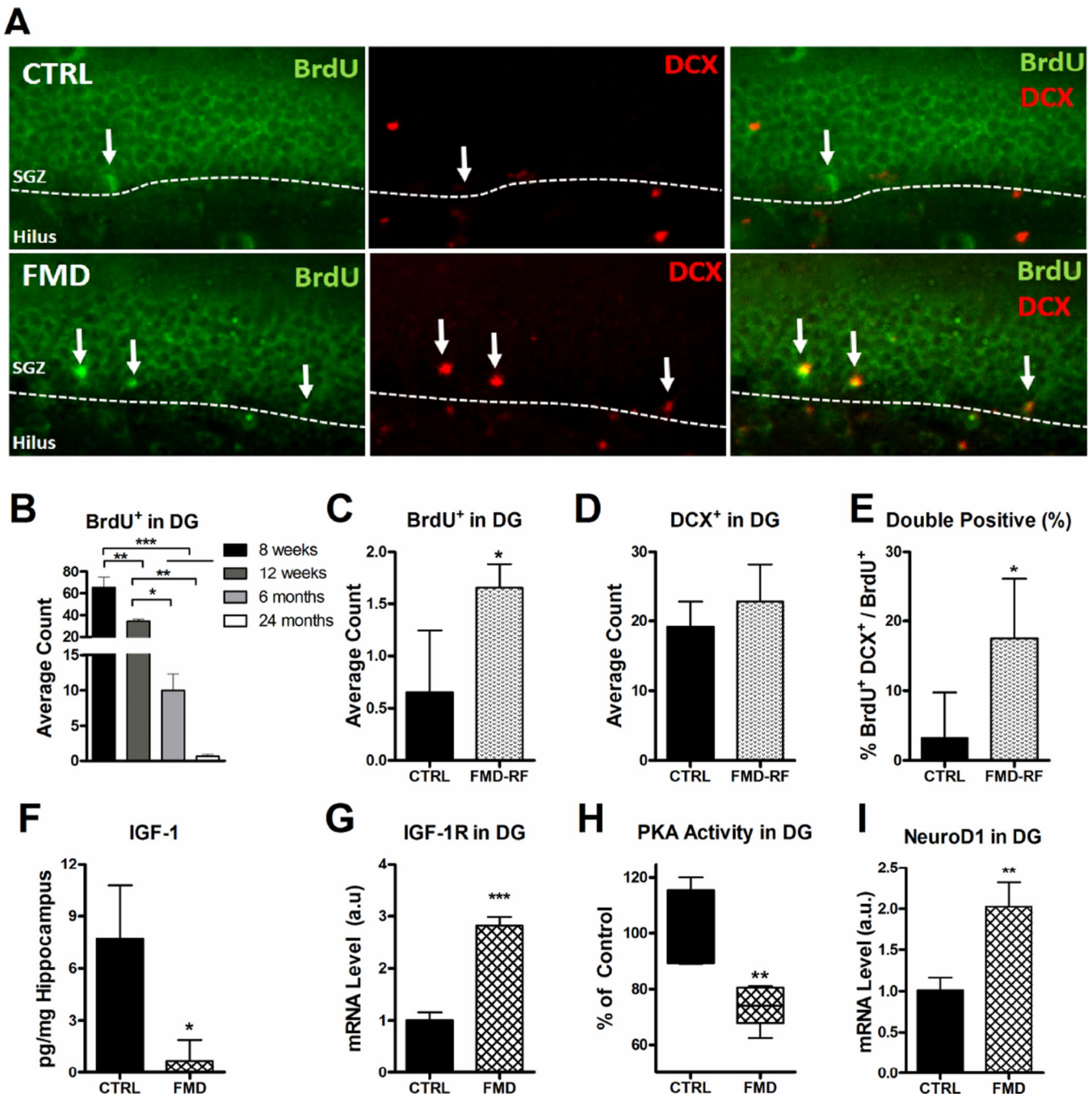

Figure 4. Periodic FMD cycle promotes adult neurogenesis

A) Hippocampal immunohistochemistry of control (top row) and FMD (bottom row, *see Methods for details*) fed 23 months-old animals for BrdU (left panel, green), DCX (middle panel, red) and $BrdU^+$ DCX^+ (right panel). **B)** Age-dependent $BrdU^+$ cell counts in sub-granular zone of the dentate gyrus (DG) (N= 4/group) **C)** $BrdU^+$ cells in the DG at the end of the FMD (N= 4/group). **D)** DCX^+ staining in the DG in 23 months-old animals (N= 4/group). **E)** Percentage of double-positive $BrdU^+$ DCX^+ cells in the DG (N= 4/group). **F)** Hippocampal IGF-1 level after FMD (N= 3/group). **G)** IGF-1R mRNA level in the DG (N=

3/group). **H)** PKA activity level in the DG (N= 5/group). **I)** NeuroD1 mRNA level in the DG (N= 3/group). All data are expressed as the mean ± SEM.

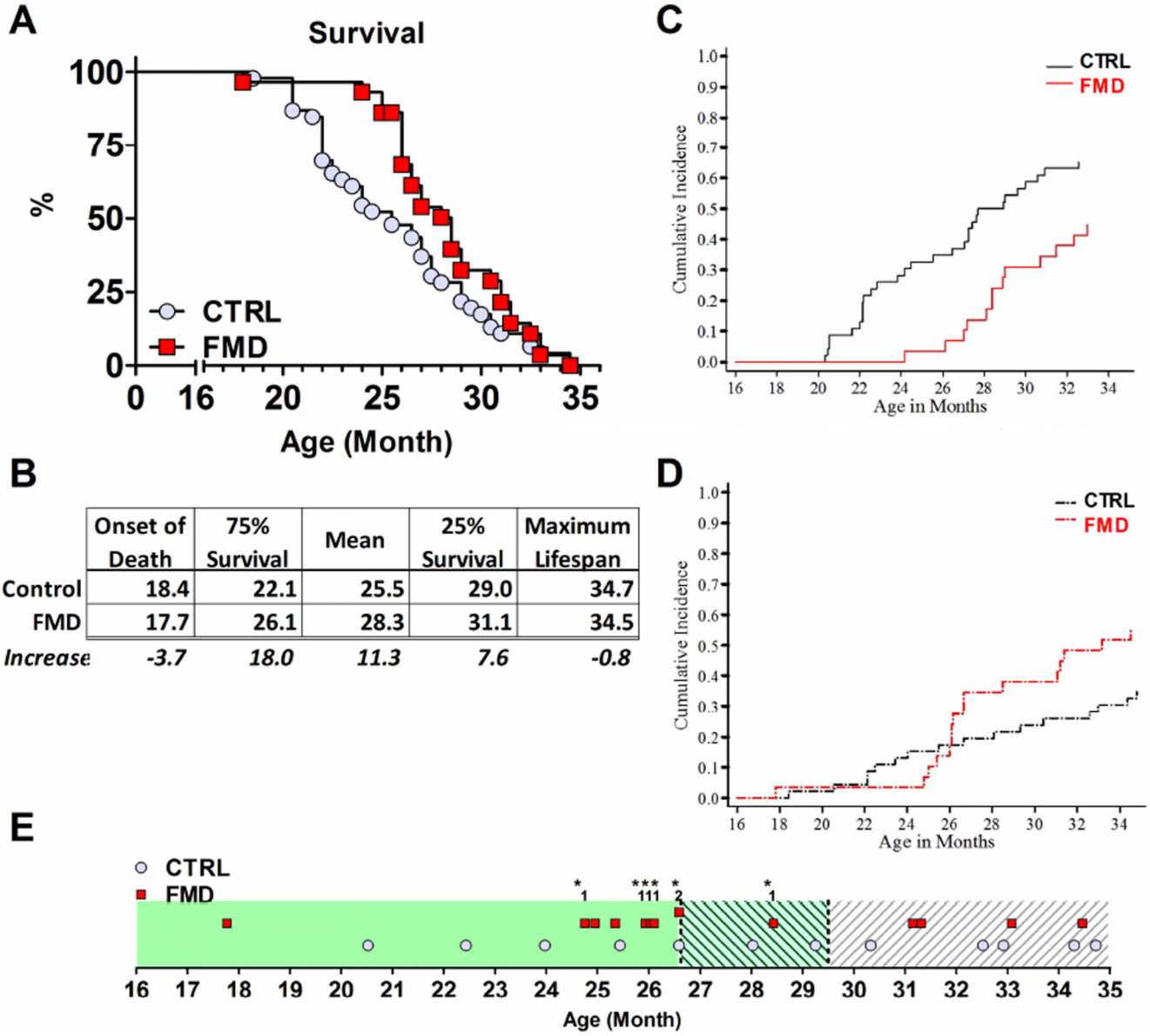

	Onset of Death	75% Survival	Mean	25% Survival	Maximum Lifespan
Control	18.4	22.1	25.5	29.0	34.7
FMD	17.7	26.1	28.3	31.1	34.5
% Increase	*-3.7*	*18.0*	*11.3*	*7.6*	*-0.8*

Figure 5. Periodic FMD cycle increase median lifespan but do not affect maximum lifespan

A) Kaplan-Meier survival curve for control and FMD cohort (N= 46 and 29, respectively). **B)** Overview for onset of death, 75%-, median-, 25%- and maximum lifespan in months with % change. **C)** Cumulative incidence rates of deaths associated with neoplasia. **D)** Cumulative incidence rates of deaths not associated with neoplasia. **E)** Overview over the date of death not associated with neoplasms. The change from the 4 day FMD to 3 day FMD is indicated by the green shaded area at 26.6 month. The stop of the 3 day FMD and switch to the *ad lib* control diet after 6 FMD cycles is indicated by the white shaded area. Numbers over the red squares indicate the number of animals deceased on the particular date, asterisk indicates that death during the FMD regime or within 3 days of refeeding. All data are expressed as the mean ± SEM.

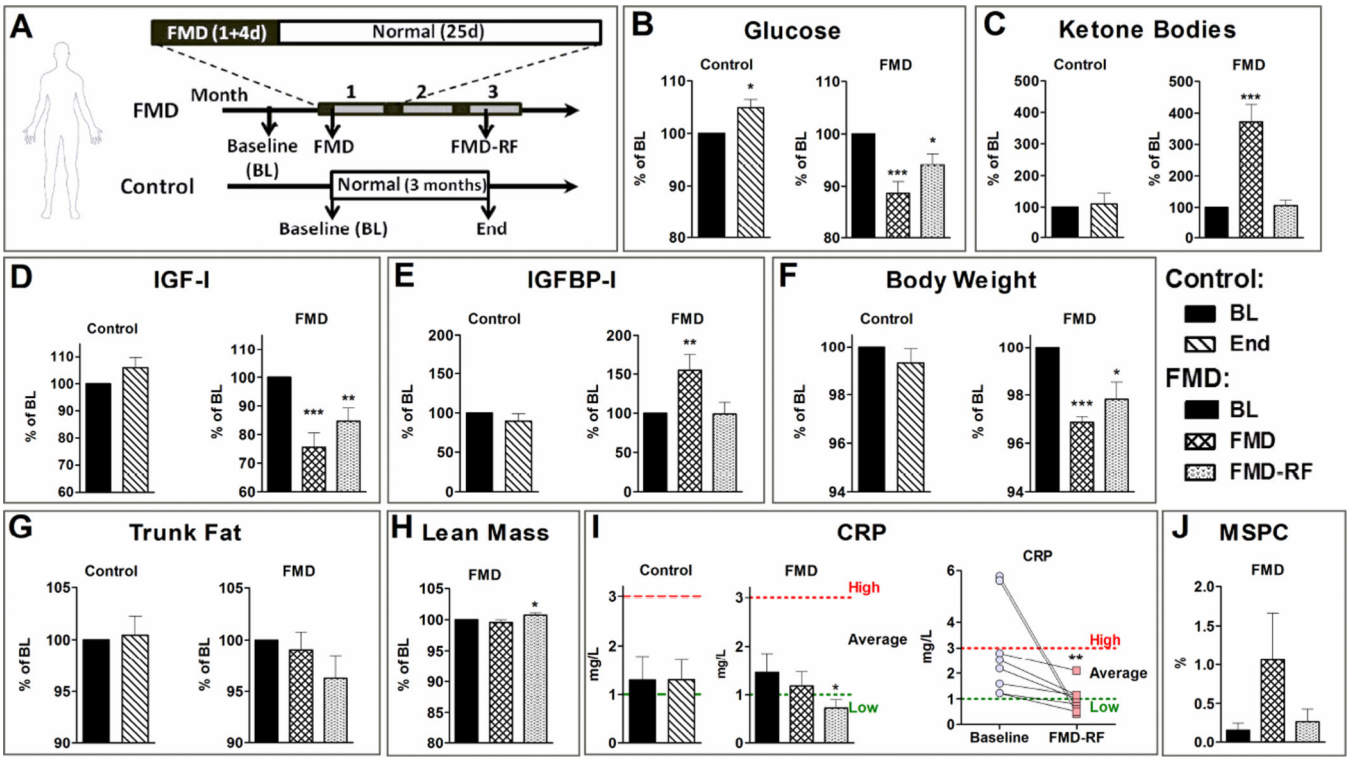

Figure 6. Effects of a human adapted FMD regimen in a pilot clinical trial

A) Subjects were randomized to either the Fasting Mimicking Diet (FMD) or a control group. Subjects in the FMD cohort consumed the FMD for 5 consecutive days every month for 3 months and returned to normal diet in-between FMDs. Control subjects continued their normal diet. Measurements were performed prior to the diet (Baseline), immediately after the first FMD cycle (FMD) and during the recovery period after the 3rd cycle (FMD-RF). Subjects in the control group were evaluated within the same time frame as the FMD-RF subjects (End). **B)** Glucose (N= 19). **C)** β-hydroxybutyrate (FMD N= 19, Control N= 18). **D)** IGF-I (FMD N= 19, Control N= 18) and **E)** IGFBP-I (FMD N= 19, Control N= 17). **F)** Body weight (N= 19). **G)** Trunk fat (FMD N= 18, Control N= 19) and **H)** Lean body mass evaluated by dual energy x-ray absorptiometry. **I)** C-reactive protein (CRP; FMD N= 19, Control N= 18) levels of all subjects (left panels) and subjects in the average or high risk group for heart disease (N= 8; right panel). **J)** Percentage of lin^{-}CD184^{+}CD45^{-} mesenchymal stem/progenitor cells (MSPC) in the peripheral blood mono-nucleated cell population (FMD N= 16, Control N= 14). All data are expressed as the mean ± SEM.